JBC RESEARCH ARTICLE

Molecular determinants of phospholipid treatment to reduce intracellular cholesterol accumulation in NPC1 deficiency

Received for publication, August 12, 2024, and in revised form, September 30, 2024 Published, Papers in Press, October 11, 2024,
https://doi.org/10.1016/j.jbc.2024.107889

Shikun Deng[1,‡], Ting-Ann Liu[1,‡], Olga Ilnytska[1,2], Tamara Allada[1], Angelina Fomina[1], Nancy Lin[1,2], Valentina Z. Petukhova[3], Koralege C. Pathmasiri[3], Kiran Chinthapally[4], Brian S. J. Blagg[4], Brandon L. Ashfeld[4], Stephanie M. Cologna[3], and Judith Storch[1,2,*]

From the [1]Department of Nutritional Sciences, and [2]Rutgers Center for Lipid Research, Rutgers University, New Brunswick, New Jersey, USA; [3]Department of Chemistry, University of Illinois Chicago, Chicago, Illinois, USA; [4]Warren Center for Drug Discovery and Development, and Department of Chemistry and Biochemistry, University of Notre Dame, Notre Dame, Indiana, USA

Reviewed by members of the JBC Editorial Board. Edited by Henrik Dohlman

Niemann-Pick type C (NPC) disease, caused by mutations in the *NPC1* or *NPC2* genes, leads to abnormal intracellular cholesterol accumulation in late endosomes/lysosomes. Exogenous enrichment with lysobisphosphatidic acid (LBPA), also known as bis-monoacylglycerol phosphate, either directly or *via* the LBPA precursor phosphatidylglycerol (PG), has been investigated as a therapeutic intervention to reduce cholesterol accumulation in NPC disease. Here, we report the effects of stereoisomer configuration and acyl chain composition of LBPA on cholesterol clearance in NPC1-deficient cells. We find that S,R, S,S, and S,R LBPA stereoisomers behaved similarly, with all 3 compounds leading to comparable reductions in filipin staining in two NPC1-deficient human fibroblast cell lines. Examination of several LBPA molecular species containing one or two monounsaturated or polyunsaturated acyl chains showed that all LBPA species containing one 18:1 chain significantly reduced cholesterol accumulation, whereas the shorter chain species di-14:0 LBPA had little effect on cholesterol clearance in NPC1-deficient cells. Since cholesterol accumulation in NPC1-deficient cells can also be cleared by PG incubation, we used nonhydrolyzable PG analogs to determine whether conversion to LBPA is required for sterol clearance, or whether PG itself is effective. The results showed that nonhydrolyzable PG species were not appreciably converted to LBPA and showed virtually no cholesterol clearance efficacy in NPC1-deficient cells, supporting the notion that LBPA is the active agent promoting late endosome/lysosome cholesterol clearance. Overall these studies are helping to define the molecular requirements for potential therapeutic use of LBPA as an option for addressing NPC disease.

Niemann-Pick type C (NPC) disease is caused by mutations in the *NPC1* or *NPC2* genes that lead to dysfunction of Niemann-Pick C1 (NPC1) or C2 (NPC2) proteins (1, 2), resulting in abnormal intracellular cholesterol accumulation in late endosomes/lysosomes (LEs/LYs) (3). Lysobisphosphatidic acid (LBPA), also known as bis-monoacylglycerol phosphate or BMP, is highly enriched the LE/LY compartment (4, 5), and treating cells with anti-LBPA antibodies leads to cholesterol accumulation in the LE/LY, similar to the NPC phenotype (6, 7). LBPA levels are increased in NPC disease cells as well as in many other lysosomal storage disorders. Interestingly, further enrichment with exogenous LBPA was shown to reverse the cholesterol accumulation in NPC1 disease cells, suggesting that the increased LBPA levels noted in untreated NPC1-deficient cells and other lysosomal storage disorder cells may be a compensatory response to aberrant accumulation of cholesterol and other lipids (8, 9). LBPA was initially discovered as a structural isomer of phosphatidylglycerol (PG) (10) and later identified as an enzymatic product of PG *in vivo* (11). Recent studies have indicated that the biosynthetic pathway from PG to LBPA appears to include the lysosomal phospholipase A2 (PLA2G15) and transacylase activities as well as the enzyme BMP synthase/CLN5, which generates LBPA from 2 mol of lysophosphatidylglycerol (LPG) (11–14).

In previous studies, we showed that LBPA dramatically increases the rate of cholesterol transfer between the NPC2 protein and model membranes (15–17), and further demonstrated that LBPA directly interacts with the hydrophobic knob of the NPC2 protein and facilitates its actions in cholesterol transport out of the LE/LY compartment (9). Incubation with PG, the precursor of LBPA, leads to cholesterol clearance in several NPC1-deficient cell models and a mouse model of NPC1 disease *via* mechanisms including the stimulation of autophagic flux, and increasing exosomal egress (9, 18, 19). We have interpreted these cellular effects of PG incubation as being secondary to its conversion to LBPA, but this was not directly tested.

NPC1 disease makes up 95% of NPC cases, while NPC2 mutations are responsible for the remaining 5% (20, 21). We found that LBPA enrichment failed to reverse the cholesterol accumulation in NPC2-deficient cells owing to the obligate NPC2–LBPA interaction, but was remarkably effective in stimulating cholesterol clearance in NPC1-deficient cells (9). To explore the potential use of PG and LBPA phospholipids as therapeutics for NPC1 disease, here we addressed several

‡ These authors contributed equally to this work.
* For correspondence: Judith Storch, storch@sebs.rutgers.edu.

unknown aspects of their metabolism and efficacy. In particular, using nonhydrolyzable PG analogs, we questioned our assumption that PG must be converted to LBPA for cholesterol clearance to occur, asking whether PG itself can lead to cholesterol clearance. We also investigated whether the stereoisomer configuration of LBPA is important for effective cholesterol clearance in NPC1-deficient cells. Finally, since we and others have shown that cellular LBPA is markedly enriched with polyunsaturated fatty acyl chains (18, 19, 22–24), we examined the effects of the acyl chain composition of LBPA on its ability to promote cholesterol clearance in NPC1-deficient human cells.

Results

Ester bonds replaced with alkyl ether linkages inhibit PG conversion to LBPA and reduce the effectiveness of cholesterol clearance in NPC1-deficient cells

To determine whether the therapeutic effects of PG on cholesterol clearance in NPC1-deficient cells are dependent on conversion to its metabolite LBPA, we used two human fibroblast cell lines harboring mutations in the NPC1 gene and exhibiting the hallmark cholesterol accumulation of NPC disease. The GM03123 fibroblast is a heterozygote mutant containing a P237S mutation in one allele of the NPC1 gene and a second allele with an I1061T mutation; the GM18453 cell line is homozygous for the I1061T mutation. NPC1 KO HeLa cells were generated in our lab using an NPC1 CRISPR-Cas9 KO construct as described (9). Cells were treated with liposomes prepared by sonication of di-oleoyl-PG or nonhydrolyzable analogues of PG, as descried under Experimental Procedures. The nonhydrolyzable PGs have one or two ester bonds replaced with alkyl ether linkages: KC-45, with both the sn1 and sn2 ester bonds replaced; KC-46, with the sn1 ester bond replaced; and KC-47, with the sn2 ester bond replaced (Fig. 1). We hypothesized that the alkyl ether linkages would be stable toward phospholipase activity, which would block the hydrolysis of PG and thus reduce LBPA production, and would therefore not be effective in clearing cholesterol in NPC1-deficient cells.

In agreement with our previous findings (9, 18, 19), lipidomic analysis showed that the exogenous treatment of NPC1$^{-/-}$ HeLa cells with di-18:1-PG markedly increased the levels of LBPA species containing 18:1 acyl chains, with many-fold increases found not only in di-18:1 LBPA but also in 18:1-16:1, 18:1-18:2, 18:1-20:4, and 18:1-22:6 LBPA species. In contrast, incubation with any of the three nonhydrolyzable PG compounds resulted in little or no increases in LBPA levels compared to control untreated cells, with the exception of 18:1-16:1-LBPA, which showed about half as much enrichment as found with dioleoylphosphatidylglycerol (DOPG) treatment but was nevertheless higher in analog-treated cells relative to untreated control cells. The levels of di-22:6-LBPA appeared to be somewhat reduced after DOPG or nonhydrolyzable PG analog treatments relative to untreated controls. Surprisingly, little or no differences in LBPA levels were found following incubation with the three analogs; our initial expectation was that blockage of the sn-2 linkage would lead to lower LBPA production than blockage of the sn-1 linkage, owing to the involvement of PLA2 activity in LBPA generation (25) (Fig. 2*A*).

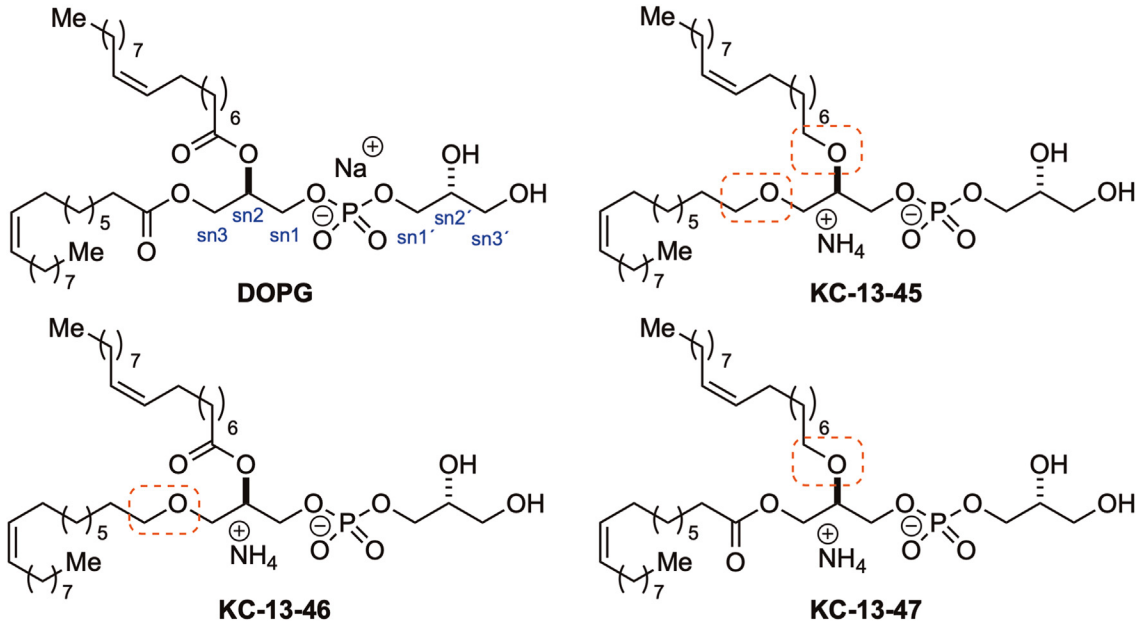

Figure 1. Molecular structure of DOPG and nonhydrolyzable PGs. DOPG: (*R*)-2,3-bis(oleoyloxy)propyl (2-(trimethylammonio)ethyl) phosphate; di-oleoyl-phosphatidylglycerol. KC-13-45: ammonium (*R*)-2,3-bis(((*Z*)-octadec-9-en-1-yl)oxy)propyl ((*R*)-2,3-dihydroxypropyl) phosphate, with sn-1 and sn-2 ester bonds replaced by ether bonds. KC-13-46: ammonium (*R*)-2,3-dihydroxypropyl ((*R*)-3-(((*Z*)-octadec-9-en-1-yl)oxy)-2-(oleoyloxy)propyl) phosphate, with the sn-1 ester bond replaced by an ether bond. KC-13-47: ammonium (*R*)-2,3-dihydroxypropyl ((*R*)-2-(((*Z*)-octadec-9-en-1-yl)oxy)-3-(oleoyloxy)propyl) phosphate, with the sn-2 ester bond replaced by an ether bond. DOPG, dioleoylphosphatidylglycerol; PG, phosphatidylglycerol.

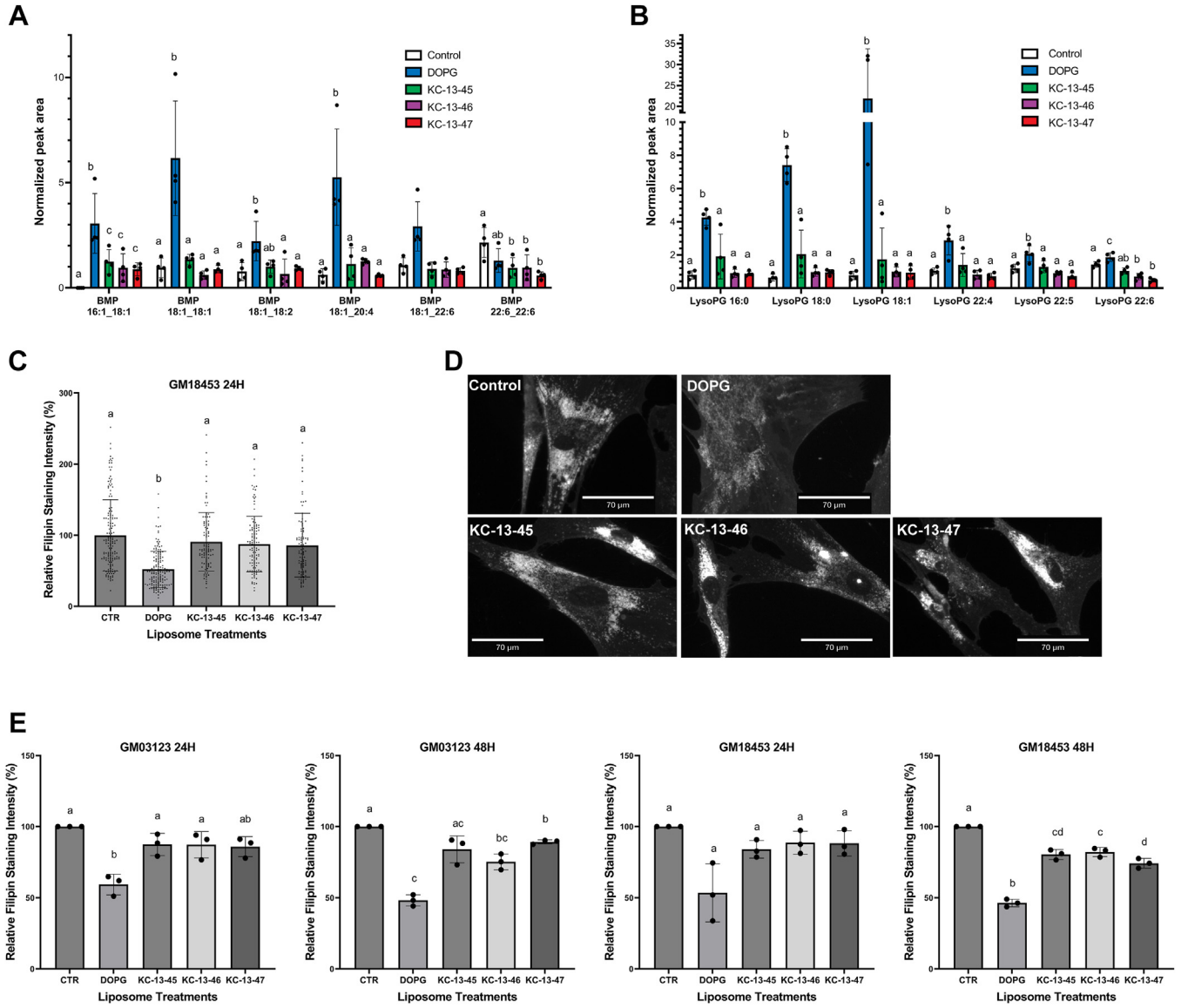

Figure 2. Ester bonds replaced with alkyl ether linkage inhibit PG conversion to LBPA and reduce the efficacy of cholesterol clearance in NPC1$^{-/-}$ cells. *A*, lipidomic analysis of LBPA species levels in NPC1-deficient HeLa cells treated with 100 uM DOPG, KC-13-45, KC-13-46, or KC-13-47 for 24 h. Peak area of each lipid is normalized to the peak area of a deuterated lipid internal standard. *B*, lipidomics analysis of LysoPG species levels in NPC1-deficient HeLa cells treated with 100 uM PG, KC-13-45, KC-13-46, or KC-13-47 for 24 h. *C*, representative experiment showing quantification of filipin intensity in NPC1-deficient human fibroblast cell line GM18453 treated with 100uM PG, KC-13-45, KC-13-46, and KC-13-47 for 24 h. Each point represents the fluorescent intensity of a single cell. N = 120 to 150 cells/condition. *D*, representative epifluorescent images of NPC1-deficient human fibroblasts GM03123 treated with 100uM DOPG, KC-13-45, KC-13-46 and KC-13-47 for 24 h. *E*, quantification of data from three independent experiments in NPC1-deficient human fibroblast cell lines GM03123 and GM18453, treated with 100 uM PG, KC-13-45, KC-13-46, or KC-13-47 for 24 or 48 h. Data in B and D are shown as mean ± SD. Different letters indicate significant differences analyzed using one-way ANOVA, at $p < 0.05$ or below. LBPA, lysobisphosphatidic acid; NPC1, Niemann-Pick type C 1; PG, phosphatidylglycerol.

We also assessed the LysoPG species (Fig. 2*B*) and detected lysoPG with 16:0, 18:0, 18:1, 22:4, 22:5, and 22:6 acyl chains. The incubation with DOPG resulted in an approximately 30-fold increase in 18:1-LysoPG and smaller but significant increases in 18:0-LysoPG, 16:0-LysoPG, 22:4-LysoPG, 22:5-LysoPG, and 22:6-LysoPG (Fig. 2*B*).

We then tested the nonhydrolyzable PG analogs in cholesterol laden NPC1-deficient fibroblasts. Cholesterol clearance by the analogs, over 24 or 48 h, was significantly lower than incubation with native PG, as observed by filipin staining intensities (Fig. 2, *C* and *D*). Treatment of both GM03123 and GM18457 NPC1-deficient fibroblasts with DOPG led to the expected ≈50% reduction in filipin staining, indicating cholesterol clearance from the LE/LY compartment. By contrast, treatment with the nonhydrolyzable PG compounds did not lead to any appreciable reduction in filipin staining in either cell line at 24 h. At 48 h a 10 to 15% decrease in filipin staining was observed in the GM 18453 cells. Thus, all the analogues were markedly less effective than DOPG in both cell lines and at both time points. If PG itself had an effect, we might have expected to observe reduced cholesterol levels in NPC1$^{-/-}$ cells upon incubation with the analogues. Therefore,

the results strongly suggest that PG must be metabolized to LBPA to effectively promote cholesterol clearance in NPC1$^{-/-}$ cells, and that PG itself is largely ineffective.

LBPA(BMP) stereoisomerism does not influence cholesterol clearance efficacy in NPC1-deficient cells

We previously reported that the exogenous enrichment of LBPA increases cholesterol egress from the LE/LY compartment in NPC1$^{-/-}$ cells (9, 18, 19). In these prior studies, we utilized the LBPA (S,R) stereoisomer. LBPA exists in other stereoconfigurations, namely (S,S) and (R,R), and in humans, LBPA is thought to primarily exist in the (S,S) stereoconfiguration (26, 27). Thus the question arises as to whether the stereoconfiguration of LBPA would influence its effectiveness in cholesterol clearance in NPC-deficient cells.

NPC1-deficient fibroblasts (GM03123 and GM18453) were incubated with liposomes prepared by sonication of (S,R), (S,S), or (R,R) di-18:1 LBPA stereoisomers as described under Experimental procedures, for 24 or 48 h. In contrast to the untreated controls and in agreement with all our prior results, exogenous enrichment with LBPA (S,R) reduced cholesterol accumulation in LE/LY of NPC1-deficient fibroblasts. We found that the (S,S) and (R,R) LBPA stereoisomers resulted in cholesterol reductions comparable to that of the (S,R) configuration. In all cases, NPC1-deficient fibroblasts supplemented with (S,S), (S,R), or (R,R) LBPA showed an approximately 40% reduction in filipin staining (Fig. 3). These results indicate that that the stereoconfiguration of di-18:1 LBPA does not influence its effectiveness in clearing cholesterol in NPC1-deficient fibroblasts.

The effects of LBPA acyl chain composition on cholesterol clearance in NPC1-deficient cells

Previous LC-MS analyses of LBPA molecular species in cells supplemented with di-18:1-PG showed a marked increase in diC18:1-LBPA but also significant increases in LBPA-containing polyunsaturated fatty acids including arachidonic acid (20:4) and particularly docosahexaenoic acid (22:6) (18, 19, 23, 24). We wondered whether the enrichment in polyunsaturated fatty acid would modulate the ability of LBPA enrichment of reduce LE/LY cholesterol levels. We therefore compared the effectiveness of LBPA molecular species synthesized to contain one oleate chain and a second acyl chain of 16:0, 18:1, 18:2, 20:4, or 22:6 (Fig. 4*A*), in modulating cholesterol accumulation in NPC1-deficient cells (28).

GM18453 NPC1$^{-/-}$ fibroblasts were incubated with increasing amounts of liposomes prepared by sonication of LBPA: phosphatidylcholine (PC) (1:1 mol/mol) using LBPA molecular species 18:1-18:1, 18:1-18:2, 18:1-20:4, 18:1-22:6, or 18:1-16:0 LBPA, as described under Experimental procedures, for 48 h. Cell viability was assessed in the NPC1-deficient fibroblasts following a 48-h incubation with the LBPA molecular species at total phospholipid concentrations of 200 μM and 400 μM (PC:LBPA 1:1 mol:mol); no effects on cell growth were found (Fig. 4*B*). Forty-eight hours treatments with the all the 18:1-x LBPA species tested resulted in a significant diminution in filipin staining, indicating cholesterol clearance from the LE/LY compartment. No significant differences were observed between the treatment groups, indicating that LBPA containing all these long-chain fatty acids (≥16C) were functionally competent for sterol clearance. (Fig. 4, *C* and *D*).

Since our previous kinetics studies of cholesterol transfer between NPC2 and model membranes showed lower sterol transfer rates with LBPA containing shorter chain 14:0 fatty acids (16), we compared cholesterol clearance in GM03123 NPC1$^{-/-}$ fibroblasts incubated with 100 μM of di-18:1, 18:1-18:2, or di-14:0-LBPA liposomes. A 24 h treatment resulted in a significant diminution in luminesce in the di-18:1 and 18:1-18:2-LBPA–treated cells, whereas cholesterol clearance with di-14:0 LBPA treatment was significantly less than with the longer unsaturated chain LBPAs, as shown in Fig. 4. The results support an acyl chain species-dependent modulation of cholesterol clearance by LBPA, with the shorter chain saturated myristoyl-LBPA less effective than the LBPA species with longer and unsaturated acyl chains. At all levels tested over the times tested, however, we found little difference between monounsaturated relative to polyunsaturated long acyl chains on sterol egress from the LE/LY compartment.

Discussion

PG has long been known as the major and perhaps sole phospholipid precursor of LBPA (24, 29–31). In previous studies, we demonstrated that PG treatment leads to cholesterol clearance in NPC1-deficient cultured cells and in Purkinje neurons of NPC-deficient mice (9, 18, 19). It is thought that a step in the conversion of PG to LBPA involves lysosomal hydrolysis of the acyl ester bond, likely at the sn-2 position (11). There is abundant evidence in the literature for hydrolysis of PG by PLA2 as an initial step in the metabolic conversion of PG to LBPA (13, 14) and the lysosomal PLA2, which is active at acidic pH, was recently identified as playing a role in the generation of LBPA from PG (32). Interestingly, it has now been shown that LBPA/BMP can in fact be synthesized from 2 mol of lyso PG *via* a BMP synthase, the product of the CLN5 gene (12). Thus, it is reasonable that both PG and LBPA enrichment in NPC1-deficient cells can contribute to endolysosomal cholesterol clearance. However, what remains uncertain is whether the effects are due solely to PG conversion to LBPA, or whether sterol clearance can be stimulated by PG itself. To differentiate between these possibilities, we used nonhydrolyzable PG analogs in which the ester bonds are replaced with alkyl ether linkages to block phospholipase hydrolysis and thus LBPA production. Indeed, lipidomics analysis of NPC1$^{-/-}$ HeLa cells treated with these phospholipid analogs demonstrated that ester bond replacement with alkyl ether linkages markedly reduced conversion to LBPA, leading to dramatically lower LBPA levels than cells treated with native PG. Little LBPA production was found following incubation with compounds where both ester bonds were replaced, or when only sn-1 or sn-2 linkages were nonhydrolyzable. Surprisingly, there was little difference in LBPA production between PG analogs with sn-1 or sn-2 alkyl ether linkages. This

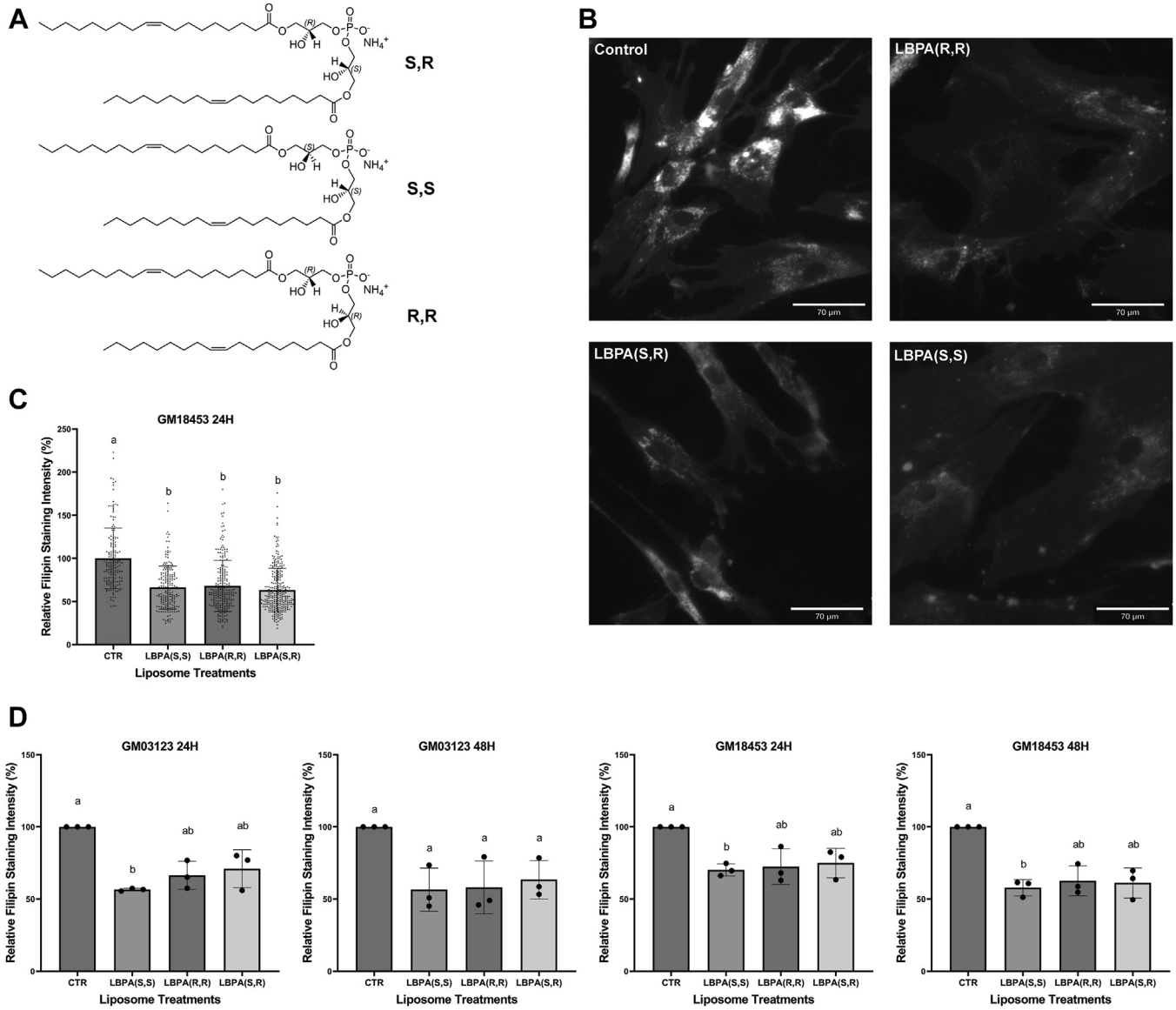

Figure 3. LBPA (BMP) stereoisomers display equivalent cholesterol clearance efficacy in NPC1-deficient cells. *A*, structures of di-oleoyl LBPA stereoisomers. *B*, representative epifluorescent images in NPC1-deficient human fibroblasts GM03123 treated with 100 uM LBPA (S,S) (S,R) or (R,R) for 24 h. *C*, representative experiment showing quantification of filipin intensity in NPC1-deficient human fibroblast cell line GM18453 treated with 100 uM LBPA (S,S) (S,R) or (R,R) for 24 h. Each point represents the fluorescent intensity of a single cell. N = 120 to 150 cells/condition. *D*, data from three independent experiments in NPC1-deficient human fibroblast cell line GM03123 and GM18453 treated with 100uM LBPA (S,S) (S,R) (R,R) for 24 or 48 h. Data in C and D are shown as mean ± SD. Different letters indicate significant differences analyzed using one-way ANOVA, at $p < 0.05$ or below. LBPA, lysobisphosphatidic acid; NPC1, Niemann-Pick type C 1.

may indicate that an alklyl linkage in either position alters substrate structure such that remaining ester bonds might not be accessible for hydrolysis by phospholipase enzymes. Cholesterol clearance studies showed that the positive control DOPG effectively led to sterol egress from the LE/LY, while the three types of nonhydrolyzable PGs had little to no effect on cholesterol clearance in NPC1-deficient fibroblasts. The clear agreement between filipin intensities and lipidomics analysis suggests that PG conversion to LBPA is necessary, and that LBPA is likely the active species involved in clearing cholesterol from NPC1-deficient cells following PG administration. As noted above, LPG is thought to be an intermediate in the conversion of PG to LBPA. This is supported by the observed robust elevations in LPG species seen following PG incubations. While 18:1-LPG was the major species found at 24 h of incubation with di-18:1-PG, the increases in other LPG species may suggest the presence of acyl group rearrangement and acyltransferase activities.

LBPA can exist in several stereoconfigurations. We previously showed that the dramatic stimulation by LBPA of cholesterol transfer rates between purified NPC2 and model membranes, was virtually identical for S,R, S,S and R,R stereoisomers of LBPA (16). Here, we tested the effects of these LBPA stereoisomers on the clearance of intracellular cholesterol accumulation in NPC1-deficient fibroblasts. In keeping with the findings using membrane vesicles, our results

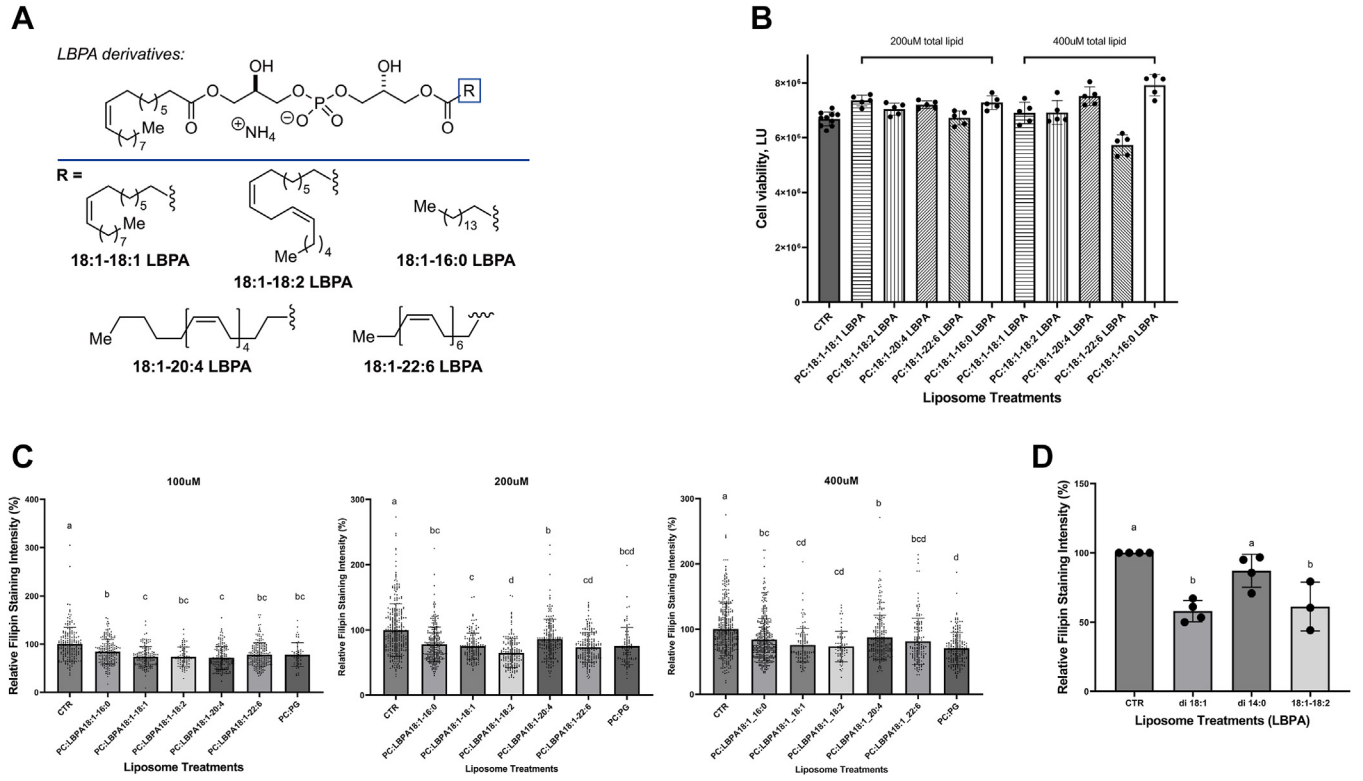

Figure 4. Effects of LBPA (BMP) with different acyl chain composition on cholesterol clearance efficacy in NPC1-deficient cells. *A*, structures of LBPA (BMP) derivatives. *B*, NPC1-deficient GM18453 fibroblast cell viability following 48 h incubation with increasing concentrations of LBPA molecular species. *C*, NPC1$^{-/-}$ GM18453 fibroblasts treated with 100 uM, 200 uM, or 400 uM of 1:1 mol:mol PC:LBPA for 48 h. *D*, data from 3 to 4 independent experiments in NPC1-deficient human fibroblast cell line GM03123 treated with 100 uM di-18:1, di-14:0, or 18:1-18:2 LBPA for 24 h. N = 4 except for 18:1, 18:2-LBPA, N = 3. Data shown as mean ± SD. Different letters indicate significant differences analyzed using one-way ANOVA, at $p < 0.05$ or below; similar letters indicate no significant differences. BMP, bis-monoacylglycerol phosphate; LBPA, lysobisphosphatidic acid; NPC1, Niemann-Pick type C 1; PC, phosphatidylcholine.

demonstrate that the 3 LBPA stereoisomers led to similar reductions in filipin staining in two NPC1-deficient fibroblast cell lines. Such correspondence between the regulation of NPC2 sterol transfer rates in simple systems consisting only of purified NPC2 and model membranes, and its regulation of cholesterol clearance in NPC1-deficient cells (which have WT levels of NPC2), is in keeping with prior structure-function studies of NPC2 wherein point mutations in NPC2 that severely reduce its rate of cholesterol transfer to liposomes, are also unable to rescue the cholesterol accumulation phenotype of NPC2$^{-/-}$ human cells (9, 17). It is worth noting in this regard that LBPA enrichment, either directly or *via* PG treatment, does not work in most NPC2-deficient cells since the mechanism of LBPA action in sterol clearance involves an obligate interaction with the hydrophobic knob domain of NPC2 (9). In the present studies, we find that, as seen in the simple model membrane system, the stereoisomer configuration of LBPA does not appear to affect its ability to clear cholesterol in NPC1-deficient cells. LBPA is thought to exist in cells as the S,S isomer (11, 27, 33) and evidence also suggests that LBPA is long-lived relative to other phospholipids, including its precursor PG (34, 35). It is possible that the S,S isomer is more stable to the acidic environment of the LE/LY compartment, and perhaps more resistant to phospholipase hydrolysis. A recent report shows that all three stereoisomers of LBPA are over an order of magnitude more stable than PG following their addition to cell lysates, with the S,S isomer somewhat more stable than the other two but still markedly more stable than PG (36). In the present studies, the cholesterol clearance is observed at 24 and 48 h of liposome incubation, thus any differences in isomer stability are not functionally manifested. On a longer time scale it is possible that differential stability might lead to differences in isomer efficacy, however the present results indicate that the effectiveness of each of the LBPA isomers *in situ* is virtually identical. In addition to stereoisomers, acyl attachment site confers structural isomers of LBPA. The three stereoisomers compared herein and by others (36) were obtained from Avanti Polar Lipids and all have 3,3′ acyl attachment sites. It is thought that *in vivo* the 2,2′ configuration is predominant and that it preferentially promotes formation of ILVs within the LE/LY compartment (5). One possibility is that 2,2′ LBPA species may prove even more effective at cholesterol clearance in NPC1 deficiency, and this remains to be tested. It is worth noting that incubation of NPC1-deficient cells with PG, the LBPA precursor, allows for formation of the biologically relevant species *in situ*, and has been the primary mode of LBPA enrichment in our prior studies (9, 17–19).

LBPA is known to be enriched in long acyl chains, particularly the abundant 18:1 and, interestingly, the

polyunsaturated docosahexaenoic acid, 22:6 (22, 23). In agreement with our previous results (18, 19), we found that cell incubation with DOPG leads not only to an expected increase in di-18:1-LBPA but also to marked enrichment in LBPA with 22:6 chains. The functional reason for this enrichment is not definitively known but is speculated to involve the role of LBPA in membrane curvature and fusion, and formation of intraluminal vesicles within the late endosomal (also termed multivesicular bodies) compartment (5, 37, 38). We asked whether LBPA species with different acyl chain compositions, in particular including 22:6, would differentially clear cholesterol in NPC1-deficient cells. We found that under the conditions tested all LBPA molecular species examined (18:1-18:1, 18:1-18:2, 18:1-20:4, 18:1-22:6, and 18:1-16:0 LBPA), containing long acyl chains (≥16C), promoted similar clearance of cholesterol from the LE/LY compartment. Only di-14:0-LBPA was found to have substantially less cholesterol clearance activity. This is in keeping with model systems studies in which we had found that the NPC2 cholesterol transfer rate was ∼60% slower for membranes containing di-14:0-LBPA than di-18:1-LBPA (16). As with the above-mentioned results using LBPA stereoisomers, the model membrane studies of cholesterol transport by NPC2 agree well with cell-based studies of sterol transfer in NPC1-deficient cells, underscoring the importance of the NPC2–LBPA interaction in cholesterol trafficking within the LE/LY vesicle system.

One of the mechanisms by which LBPA enrichment appears to promote cholesterol redistribution out of the LE/LY compartment in NPC1 deficiency is by stimulating autophagy (18), which is known to be reduced in NPC disease (39, 40). Several other neurodegenerative diseases are also characterized by impaired autophagy, including Alzheimer's and Parkinson's diseases, and several other lysosomal storage disorders (41–45). Neurons are highly polarized cells, and efficient clearance or recycling of varied autophagic and endocytic substrates is required for neuronal function and maintenance (46). The nervous system is thus especially vulnerable to lysosomal perturbation, therefore understanding the molecular determinants of LBPA activity in the stimulation of intracellular vesicle trafficking and cholesterol clearance may contribute to the development of therapeutics for these devastating neurological disorders.

Experimental procedures

Mammalian cell culture

NPC fibroblast cell lines with NPC1 gene mutations: GM03123 (I1061T/P237S) and GM18453 (I1061T/I1061T) were obtained from Coriell Cell Repositories (Coriell Institute). HeLa NPC1 KO cells were generated in our laboratory as previously described (McCauliff, 2019). Fibroblast cells were cultured in Minimum Essential Medium with Earle's salts (Sigma) supplemented with 15% fetal bovine serum, 1% penicillin-streptomycin solution and 1X sodium pyruvate (Gibco). HeLa NPC1 KO cells were cultured in Dulbecco's modified Eagle's medium (Gibco) supplemented with 10% FBS and 1% penicillin-streptomycin solution. All cells were below passage 15. All cell lines were maintained in 5% CO2 at 37 °C.

Preparation of liposomes and cell treatments

Liposomes were prepared by sonication as previously described (18, 47), with removal of impurities by 16,000*g* centrifugation for 30 min at 4 °C. 18:1 (Δ9-Cis) 1,2-dioleoyl-sn-glycero-3-(Phospho-rac-(1-glycerol) (PG)), di-18:1-LBPA stereoisomers: 18:1 BMP (S, R) bis(monooleoylglycero)phosphate (S, R Isomer), 18:1 BMP (S, S) sn-(3-oleoyl-2-hydroxy)-glycerol-1-phospho-sn-1'-(3′-oleoyl-2′-hydroxy)-glycerol, 18:1 BMP (R, R) sn-(1-oleoyl-2-hydroxy)-glycerol-3-phospho-sn-3'-(1′-oleoyl-2′-hydroxy)-glycerol, and L-α-PC (Egg PC) were purchased from Avanti Polar Lipids. Cells were treated with liposomes when they reached approximately 80 to 90% confluency. Prior to treatment, the medium was replaced with fresh medium. During the experiments, liposomes were added to a concentration of 100 uM unless otherwise specified. Control untreated cells were treated with the same volume of PBS.

Fixation and filipin staining

The liposome-treated fibroblasts were fixed as previously described (18). For filipin staining, the cells fixed on coverslips were stained with cholesterol-binding polyene antibiotic filipin III (*Streptomyces* Filipinensis) (Sigma) at 50 ug/ml in PBS in the dark at room temperature for 1 h, followed by incubation in the dark at 37 °C for another 1 h. After the staining, the coverslips were washed with PBS 3 times to remove excess filipin and mounted using Fluoromount G (EMS).

Fluorescence imaging and analysis

Cells for fixation were grown on glass coverslips and were then mounted on glass slides as described above. Images were taken with the epifluorescent Revolve Microscope at 20x magnification using a 4',6-diamidino-2-phenylindole filter to detect filipin staining. Fluorescence microscopy was chosen to enable assessment of the extent of accumulation of cholesterol in the perinuclear late endosome/lysosome region of the cell. Filipin is known to be photolabile, thus microscope light settings were always adjusted to ensure the absence of photobleaching (48), and when comparing different conditions for the treatments, images were all captured using identical microscope settings. Although biochemical analysis of cholesterol does not suffer from potential bleaching problems, it is well appreciated that in NPC disease cells, redistribution of cholesterol from the LE/LY, which restores normal cholesterol homeostasis, is not quantitatively accompanied by reductions in total cell cholesterol, thus examination of single cells is preferable as a measure of cholesterol clearance (19, 49, 50). Fluorescent intensities of the subcellular structure stained with filipin III were analyzed using ImageJ (https://imagej.net/) software. To quantify the relative intensity of filipin fluorescence, regions of interest were selected for the target areas and equal sized extranuclear background areas, and data were corrected for background intensity. Between 100 and 300 cells

per condition were analyzed for each experiment. Data were analyzed from 3 to 4 separate experiments by one-way ANOVA, followed by Tukey's multiple comparisons test. Significance was determined by $p < 0.05$.

Lipid extraction for lipidomics analysis of LBPA and lysoPG molecular species

Methanol (LC-MS grade), acetonitrile (LC-MS grade), chloroform (LC-MS grade), ammonium acetate (reagent grade), PMSF, sodium fluoride, sodium orthovanadate were obtained from Sigma-Aldrich. Isopropanol (LC-MS grade) were obtained from VWR international. All reagents were used as supplied unless otherwise noted. For lipid extraction, cell pellets were resuspended in 1X PBS buffer containing phosphatase inhibitors (1 mM sodium fluoride, 1 mM β-glycerophosphate, 1 mM PMSF, and 1 mM sodium orthovanadate). Resuspended cells were lysed three times by probe sonication (30% amplitude, 1 s on, 1 s off, and 10 pulses). The protein concentration of the lysed cells was measured using the Pierce bicinchoninic acid Protein Assay (Thermo Fisher Scientific). To an equivalent of 2.4 μg of protein from each sample, 1X PBS was added to the final volume of 23 μl followed by 6 μl of the 1:40 diluted SPLASH deuterated lipidomic standard (Avanti Polar Lipids, Alabaster). To each sample, 200 μl of the $CHCl_3$:MeOH (2:1, v/v) was added and incubated for 15 min at room temperature. During this incubation, samples were vigorously vortexed every 5 min. After the incubation time, 27 μl of 1 M NaCl + 0.1 M HCl was added and vortexed, followed by centrifugation at 1500 rpm for 5 min at room temperature to induce phase separation. The lower organic phase was transferred into a fresh tube. The remaining aqueous layer was re-extracted using 200 μl $CHCl_3$ solution, and the resulting organic layer was combined with the initial organic layer. Combined organic layers were dried under a vacuum and resuspended in 23 μl of methanol/$CHCl_3$ (3:1, v/v).

LC-MS and data analysis

Lipid separation was performed using an Agilent 1290 Infinity II UHPLC system outfitted with an Agilent Poroshell 120 EC-C18 column (2.1 × 100 mm, 2.7 μm). The column was maintained at 50 °C and operated at a flow rate of 0.3 ml/min. Mobile phases consisted of solvent (A) 90:10 (v/v) water:methanol with 5 mM ammonium acetate and solvent (B) 20:30:50 (v/v) acetonitrile:methanol:isopropanol with 5 mM ammonium acetate. The chromatographic gradient was as follows: 70% B at 0 to 1 min, 86% B at 3.5 to 10 min, and 100% B at 11 to 17 min at a flow rate of 0.3 ml/min. A postcolumn equilibration time of 5 min was used for all runs. Source parameters were as follows: gas temp (200 °C), drying gas (11 L/min), nebulizer (35 psi), sheath gas temp (250 °C), sheath gas flow (12 L/min), VCap (3000 V), and fragmentor (145 V). Data acquisition was performed using an Agilent 6550 quadrupole time-of-flight mass spectrometer in positive and negative ion modes *m/z* range 200 to 1700 in MS only (no fragmentation) mode. A pooled sample of equal amounts of all biological samples was analyzed using the iterative MS/MS (fragmentation) mode with a fixed collision energy of 25 eV to generate a spectral library. Data analysis: From the raw MS/MS data of the pooled sample, a fragmentation-based lipid library containing *m/z* precursors and retention times was created using Agilent Lipid Annotator software (Agilent Technologies Inc, https://www.agilent.com/en/product/software-informatics/mass-spectrometry-software/data-analysis/mass-profiler-professional-software) with the following settings: Q-Score ≥60 and mass deviation ≤10 ppm. Raw LC-MS data files were processed using Agilent Profinder software to generate extracted ion chromatograms for each lipid in the library. Each of the integrated peaks was manually reviewed for retention time and fragmentation matching. The processed data file was imported into the Mass Profiler Professional software (https://www.agilent.com/en/product/software-informatics/mass-spectrometry-software/data-analysis/mass-profiler-professional-software) as a .cef file, where all compound abundance values were baseline corrected to the median abundance for statistical analysis. GraphPad Prism software (www.graphpad.com) was used for data representation of statistical analysis results.

Synthesis of LBPA molecular species and non-hydrolyzable PG analogues

Solvents and reagents were American Chemical Society reagent grade and used without further purification unless noted below. Dimethylformamide, tetrahydrofuran (THF), dichloromethane (CH_2Cl_2), and diethyl ether were passed through a column of molecular sieves and stored under argon. All reactions were carried out in flame-dried glassware under a nitrogen atmosphere unless otherwise specified. ^{1}H NMR spectra were obtained at 400 MHz, and ^{13}C NMR spectra at 101 MHz. Chemical shifts are reported in parts per million (ppm, δ), and referenced to residual solvent or tetramethylsilane. Coupling constants are reported in Hz. Spectral splitting patterns are designated as s, singlet; d, doublet; t, triplet; q, quartet; p, pentet; m, multiplet. IR spectra were obtained using a Thermo Electron Nicolet 380 FT-IR using a silicon (Si) crystal in an attenuated total reflectance tower and reported as wavenumbers (cm^{-1}). High and low resolution electrospray ionization measurements were made with a Bruker MicroTOF II mass spectrometer. Components (*S*)-2,3-bis(((*Z*)-octadec-9-en-1-yl)oxy)propan-1-ol, (*S*)-1-hydroxy-3-(((*Z*)-octadec-9-en-1-yl)oxy)propan-2-yl oleate, and (*S*)-3-hydroxy-2-(((*Z*)-octadec-9-en-1-yl)oxy) propyl oleate were prepared using known literature procedures (51–54). LBPA derivates were synthesized according to known literature procedures (28). NMR spectra for compounds KC-13-45, KC-13-46, and KC-13-47, which were used to establish >98% purity of each sample, are provided in the Supporting information.

(R)-2,3-Dihydroxypropyl (R)-3-{[(Z)-Octadec-9-en-1-yl]oxy}-2-(oleoyloxy)propyl Phosphate (KC-13–45)

Phosphorylative coupling—To a stirred solution of 2-cyanoethyl *N*,*N*-diisopropylchlorophosphoramidite (26 mg, 0.18 mmol) in CH_2Cl_2 (1.5 ml) was added $^iPr_2NEt$ (26 μl)

and a solution of (*S*)-2,3-bis(((*Z*)-octadec-9-en-1-yl)oxy) propan-1-ol (0.074 mmol) in CH_2Cl_2 (1 ml) dropwise over 20 to 25 min at −15 °C. The reaction mixture was allowed to warm slowly from −15 °C to room temperature over 3 h. A solution of (*S*)-2,3-bis((*tert*-butyldiphenylsilyl)oxy)propan-1-ol (72 mg, 0.13 mmol) in CH_2Cl_2 (0.5 ml) and tertrazole (330 μl, 0.45 M, 0.15 mmol) were then added at 0 °C, and the mixture stirred at room temperature for 12 h. Then, ^{t}butyl hydroperoxide (54 μl, 5.5 M, 0.27 mmol) was added, and the mixture stirred at room temperature for 1 h, then diluted with saturated aqueous $Na_2S_2O_3$ (5 ml). The resulting solution was extracted with CH_2Cl_2 (2 × 5 ml), the organic layers dried (Na_2SO_4), and concentrated under reduced pressure. The resulting residue was purified by flash column chromatography eluting with hexanes/EtOAc (7:1–2.5:1) to afford (2*R*)-1-[({(*R*)-2,3-Bis[(tert-butyldiphenylsilyl)oxy]propoxy}(2-cyanoethoxy)phosphoryl)oxy]-3-{[(*Z*)-octadec-9-en-1-yl]oxy}propan-2-yl oleate (61 mg, 64%) as a colorless oil: ^{1}H NMR (400 MHz, $CDCl_3$) δ 7.64 – 7.51 (m, 8H), 7.43 – 7.30 (m, 12H), 5.34 (q, *J* = 4.3, 3.1 Hz, 4H), 4.26 – 4.16 (m, 1H), 4.14 – 4.02 (m, 4H), 3.99 – 3.93 (m, 2H), 3.62 (t, *J* = 5.3 Hz, 2H), 3.48 (dd, *J* = 5.3, 2.9 Hz, 2H), 3.38 (q, *J* = 7.0 Hz, 2H), 2.64 – 2.48 (m, 2H), 2.30 (t, *J* = 7.6 Hz, 2H), 2.03 – 1.98 (m, 8H), 1.51 (t, *J* = 6.7 Hz, 2H), 1.34 – 1.22 (m, 45H), 1.02 (s, 9H), 0.99 (s, 9H), 0.88 (t, *J* = 6.6 Hz, 6H); ^{13}C{^{1}H} NMR (101 MHz, $CDCl_3$) δ 173.0 (d, *J* = 3.0 Hz), 135.8, 135.7, 135.5, 135.4, 133.5 – 133.2 (m), 133.1, 129.9 (d, *J* = 5.4 Hz), 129.7 (d, *J* = 9.6 Hz), 127.7 (d, *J* = 4.1 Hz), 127.7, 77.2, 72.1, 71.8, 68.5, 68.3, 66.3, 63.8, 61.6, 34.2, 31.9, 29.8, 29.7, 29.5, 29.5, 29.4, 29.3, 29.2, 29.1, 29.1, 27.2, 27.2, 26.8, 26.7, 26.0, 24.8, 22.7, 19.4, 19.3, 19.2, 19.1, 14.1; ^{31}P NMR (162 MHz, $CDCl_3$) δ −1.52, −1.58; high resolution mass spectrometry (HRMS: ESI-TOF) *m*/*z* [M + H]$^+$ calcd for $C_{77}H_{121}NO_9PSi_2$ 1290.8312, found 1290.8273.

Global deprotection/ammonium salt formation—To a stirred solution of (2*R*)-1-[({(*R*)-2,3-Bis[(tert-butyldiphenylsilyl)oxy]propoxy}(2-cyanoethoxy)phosphoryl)oxy]-3-{[(*Z*)-octadec-9-en-1-yl]oxy}propan-2-yl Oleate (30 mg, 0.023 mmol; 1 equiv) in THF (3 ml) was added tetrabutylammonium fluoride trihydrate (15 equiv), and the mixture stirred at room temperature for 12 h. The reaction was concentrated under reduced pressure and the resulting residue reconstituted in 4:1 v/v $CHCl_3$/MeOH (25 ml), extracted with 8 mM aqueous ammonium acetate (15 ml), and the combined organic fractions concentrated under reduced pressure. The resulting residue was passed through an activated DOWEX-NH_4^+ resin eluting with ^{i}PrOH and then concentrated under reduced pressure. The residue was purified by flash column chromatography eluting with CH_2Cl_2/MeOH (19:1–4:1) to afford KC-13-45 (14 mg, 78%) as a colorless oil: $[\alpha]_D^{20}$ = +1.1 (*c* 0.63, $CHCl_3$); ^{1}H NMR (400 MHz, $CDCl_3$) δ 5.40 – 5.27 (m, 4H), 5.15 (q, *J* = 5.1 Hz, 1H), 3.89 (d, *J* = 23.6 Hz, 5H), 3.70 – 3.50 (m, 4H), 3.48 – 3.32 (m, 2H), 2.33 (t, *J* = 7.6 Hz, 2H), 2.01 (q, *J* = 6.4 Hz, 8H), 1.56 (dt, *J* = 29.3, 6.9 Hz, 4H), 1.38 – 1.16 (m, 44H), 0.88 (t, *J* = 6.7 Hz, 6H); ^{13}C{^{1}H} NMR (101 MHz, $CDCl_3$) δ 174.0, 130.0, 129.9, 129.7, 129.6, 77.2, 71.9, 71.8, 69.1, 67.1, 64.3, 62.9, 34.4, 31.9, 29.8, 29.8, 29.8, 29.7, 29.6, 29.6, 29.5, 29.4, 29.4, 29.3, 29.3, 29.2, 27.3, 27.2, 26.1, 25.0, 22.7, 14.1; ^{31}P NMR (162 MHz, $CDCl_3$) δ 1.38, 0.66; HRMS (ESI-TOF) *m*/*z* [M]$^-$ calcd for $C_{42}H_{80}O_9P$ 759.5545, found 759.5539.

(R)-2,3-Dihydroxypropyl (R)-2-{[(Z)-Octadec-9-en-1-yl]oxy}-3-(oleoyloxy)propyl Phosphate (KC-13-46)

Phosphorylative coupling—To a stirred solution of 2-cyanoethyl *N*,*N*-diisopropylchlorophosphoramidite (26 mg, 0.18 mmol) in CH_2Cl_2 (1.5 ml) was added ^{i}Pr$_2$NEt (26 μl) and a solution of (*S*)-1-hydroxy-3-(((*Z*)-octadec-9-en-1-yl) oxy)propan-2-yl oleate (0.074 mmol) in CH_2Cl_2 (1 ml) dropwise over 20 to 25 min at −15 °C. The reaction mixture was allowed to warm slowly from −15 °C to room temperature over 3 h. A solution of (*S*)-2,3-bis((*tert*-butyldiphenylsilyl)oxy)propan-1-ol (72 mg, 0.13 mmol) in CH_2Cl_2 (0.5 ml) and tertrazole (330 μl, 0.45 M, 0.15 mmol) were then added at 0 °C, and the mixture stirred at room temperature for 12 h. Then, ^{t}butyl hydroperoxide (54 μl, 5.5 M, 0.27 mmol) was added, and the mixture stirred at room temperature for 1 h, then diluted with saturated aqueous $Na_2S_2O_3$ (5 ml). The resulting solution was extracted with CH_2Cl_2 (2 × 5 ml), the organic layers dried (Na_2SO_4), and concentrated under reduced pressure. The resulting residue was purified by flash column chromatography eluting with hexanes/EtOAc (7:1 to 2.5:1) to afford (2*R*)-3-[({(*R*)-2,3-Bis[(tert-butyldiphenylsilyl)oxy]propoxy}(2-cyanoethoxy)phosphoryl)oxy]-2-{[(*Z*)-octadec-9-en-1-yl]oxy}propyl Oleate (61 mg, 64%) as a colorless oil: ^{1}H NMR (400 MHz, $CDCl_3$) δ 7.68 – 7.50 (m, 8H), 7.45 – 7.27 (m, 12H), 5.40 – 5.29 (m, 4H), 4.29 – 4.09 (m, 3H), 4.09 – 3.90 (m, 4H), 3.69 – 3.57 (m, 3H), 3.48 (dd, *J* = 7.8, 6.0 Hz, 2H), 2.65 – 2.47 (m, 2H), 2.29 (td, *J* = 7.6, 4.1 Hz, 2H), 2.01 (p, *J* = 6.4, 5.6 Hz, 6H), 1.69 – 1.44 (m, 6H), 1.37 – 1.21 (m, 44H), 1.02 (s, 9H), 1.00 (s, 9H), 0.88 (t, *J* = 6.7 Hz, 6H); ^{13}C{^{1}H} NMR (101 MHz, $CDCl_3$) δ 173.4, 135.8, 135.7, 135.6, 135.5, 135.5, 135.4, 133.4, 133.3, 133.2 (d, *J* = 2.0 Hz), 133.1 (d, *J* = 2.0 Hz), 130.0, 129.9, 129.8 (t, *J* = 2.0 Hz), 129.7, 127.7, 127.6, 127.6, 116.1, 77.2, 75.7 (d, *J* = 10.0 Hz), 72.1 (d, *J* = 8.0 Hz), 70.7, 68.5 (d, *J* = 4.0 Hz), 66.5 (t, *J* = 8.0 Hz), 63.7 (d, *J* = 2.0 Hz), 62.3, 61.6 (d, *J* = 3.0 Hz), 34.1, 31.9, 29.9, 29.8, 29.7, 29.7, 29.5, 29.5, 29.4, 29.3, 29.2, 29.1, 27.2, 27.1, 26.8, 26.8, 26.7, 26.0, 24.8, 22.6, 19.4, 19.4, 19.3, 19.2, 19.1, 14.1; ^{31}P NMR (162 MHz, $CDCl_3$) δ −1.51; HRMS (ESI-TOF) *m*/*z* [M + H]$^+$ calcd for $C_{77}H_{121}NO_9PSi_2$ 1290.8312, found 1290.8273.

Global deprotection/ammonium salt formation—To a stirred solution of (2*R*)-3-[({(*R*)-2,3-Bis[(tert-butyldiphenylsilyl)oxy]propoxy}(2-cyanoethoxy)phosphoryl)oxy]-2-{[(*Z*)-octadec-9-en-1-yl]oxy}propyl Oleate (35 mg, 0.023 mmol; 1 equiv) in THF (3 ml) was added tetrabutylammonium fluoride trihydrate (15 equiv), and the mixture stirred at room temperature for 12 h. The reaction was concentrated under reduced pressure and the resulting residue reconstituted in 4:1 v/v $CHCl_3$/MeOH (15 ml), extracted with 8 mM aqueous

ammonium acetate (15 ml), and the combined organic fractions concentrated under reduced pressure. The resulting residue was passed through an activated DOWEX-NH_4^+ resin eluting with ^{i}PrOH and then concentrated under reduced pressure. The residue was purified by flash column chromatography eluting with CH_2Cl_2/MeOH (19:1 to 4:1) to afford KC-13-46 (16 mg, 77%) as a colorless oil: $[\alpha]_D^{20}$ = +8.7 (*c* 0.53, $CHCl_3$); ^{1}H NMR (400 MHz, $CDCl_3$) δ 5.34 (q, *J* = 4.0, 2.6 Hz, 4H), 4.27 (dd, *J* = 11.8, 3.3 Hz, 1H), 4.10 (dd, *J* = 11.9, 6.7 Hz, 1H), 3.89 (d, *J* = 12.2 Hz, 5H), 3.63 (ddt, *J* = 20.8, 16.0, 8.6 Hz, 4H), 3.49 (q, *J* = 7.6 Hz, 1H), 2.31 (t, *J* = 7.6 Hz, 2H), 2.01 (q, *J* = 6.3 Hz, 8H), 1.56 (dt, *J* = 27.1, 7.0 Hz, 4H), 1.28 (q, *J* = 8.0, 5.8 Hz, 44H), 0.88 (t, *J* = 6.7 Hz, 6H); ^{13}C{^{1}H} NMR (101 MHz, $CDCl_3$) δ 174.0, 130.0, 129.9, 129.7, 129.6, 77.2, 71.0, 70.6, 63.9, 62.9, 34.2, 31.9, 30.0, 29.8, 29.8, 29.7, 29.6, 29.5, 29.4, 29.3, 29.2, 27.3, 27.2, 26.0, 24.9, 22.7, 14.1; ^{31}P NMR (162 MHz, $CDCl_3$) δ 0.46; HRMS (ESI-TOF) *m*/*z* $[M]^-$ calcd for $C_{42}H_{80}O_9P$ 759.5545, found 759.5548.

(R)-2,3-Bis{[(Z)-octadec-9-en-1-yl]oxy}propyl (R)-2,3-Dihydroxypropyl Phosphate (KC-13-47)

Phosphorylative coupling—To a stirred solution of 2-cyanoethyl *N*,*N*-diisopropylchlorophosphoramidite (26 mg, 0.18 mmol) in CH_2Cl_2 (1.5 ml) was added ^{i}Pr$_2$NEt (26 μl) and a solution of (*S*)-3-hydroxy-2-(((*Z*)-octadec-9-en-1-yl)oxy) propyl oleate (0.074 mmol) in CH_2Cl_2 (1 ml) dropwise over 20 to 25 min at −15 °C. The reaction mixture was allowed to warm slowly from −15 °C to room temperature over 3 h. A solution of (*S*)-2,3-bis((*tert*-butyldiphenylsilyl)oxy)propan-1-ol (72 mg, 0.13 mmol) in CH_2Cl_2 (0.5 ml) and tertrazole (330 μl, 0.45 M, 0.15 mmol) were then added at 0 °C, and the mixture stirred at room temperature for 12 h. Then, ^{t}butyl hydroperoxide (54 μl, 5.5 M, 0.27 mmol) was added, and the mixture stirred at room temperature for 1 h, then diluted with saturated aqueous $Na_2S_2O_3$ (5 ml). The resulting solution was extracted with CH_2Cl_2 (2 × 5 ml), the organic layers dried (Na_2SO_4), and concentrated under reduced pressure. The resulting residue was purified by flash column chromatography eluting with hexanes/EtOAc (7:1 to 2.5:1) to afford (*R*)-2,3-Bis{[(*Z*)-octadec-9-en-1-yl]oxy}propyl (*R*)-2,3-Bis [(tert-butyldiphenylsilyl)oxy]propyl 2-cyanoethyl phosphate (63 mg, 66%) as a colorless oil: ^{1}H NMR (400 MHz, $CDCl_3$) δ 7.67 – 7.50 (m, 8H), 7.44 – 7.27 (m, 12H), 5.40 – 5.29 (m, 4H), 4.23 (tdd, *J* = 16.4, 9.9, 5.7 Hz, 1H), 4.15 – 3.91 (m, 4H), 3.63 (h, *J* = 5.9 Hz, 2H), 3.57 – 3.46 (m, 3H), 3.40 (dtd, *J* = 13.6, 7.2, 6.6, 4.3 Hz, 3H), 2.64 – 2.48 (m, 2H), 2.01 (q, *J* = 6.4 Hz, 7H), 1.58 – 1.47 (m, 3H), 1.37 – 1.19 (m, 49H), 1.02 (s, 9H), 0.99 (s, 9H), 0.88 (t, *J* = 6.7 Hz, 6H); ^{13}C{^{1}H} NMR (101 MHz, $CDCl_3$) δ 164.0, 135.8, 135.7, 135.5, 135.4, 133.3, 133.1, 129.9, 129.8, 129.7, 127.7, 127.6, 77.2, 71.8, 70.7, 69.6, 63.8, 61.5, 31.9, 30.0, 29.8, 29.7, 29.6, 29.5, 29.5, 29.3, 27.2, 26.8, 26.7, 26.1, 26.0, 22.7, 19.2, 19.1, 14.1; ^{31}P NMR (162 MHz, $CDCl_3$) δ −1.44, −1.46; HRMS (ESI-TOF) *m*/*z* [M + Na] calcd for $C_{77}H_{122}NNaO_8PSi_2$ 1298.8338, found 1298.8312.

Global deprotection/ammonium salt formation—To a stirred solution of (*R*)-2,3-Bis{[(*Z*)-octadec-9-en-1-yl]oxy}propyl (*R*)-2,3-Bis[(tert-butyldiphenylsilyl)oxy]propyl 2-Cyanoethyl Phosphate (30 mg, 0.023 mmol; 1 equiv) in THF (3 ml) was added tetrabutylammonium fluoride trihydrate (15 equiv), and the mixture stirred at room temperature for 12 h. The reaction was concentrated under reduced pressure and the resulting residue reconstituted in 4:1 v/v $CHCl_3$/MeOH (15 ml), extracted with 8 mM aqueous ammonium acetate (15 ml), and the combined organic fractions concentrated under reduced pressure. The resulting residue was passed through an activated DOWEX-NH_4^+ resin eluting with ^{i}PrOH and then concentrated under reduced pressure. The residue was purified by flash column chromatography eluting with CH_2Cl_2/MeOH (19:1–4:1) to afford KC-13-47 (14 mg, 80%) as a colorless oil: $[\alpha]_D^{20}$ = −2.0 (*c* 0.2, $CHCl_3$); ^{1}H NMR (400 MHz, $CDCl_3$) δ 5.40 – 5.27 (m, 4H), 4.05 – 3.80 (m, 5H), 3.72 – 3.50 (m, 5H), 3.50 – 3.37 (m, 3H), 2.01 (q, *J* = 6.4 Hz, 8H), 1.53 (q, *J* = 6.8 Hz, 4H), 1.27 (q, *J* = 6.1, 4.8 Hz, 47H), 0.88 (t, *J* = 6.7 Hz, 6H); ^{13}C{^{1}H} NMR (101 MHz, $CDCl_3$) δ 129.9, 129.7, 129.7, 77.2, 71.8, 70.5, 70.2, 65.1, 31.9, 30.0, 29.9, 29.8, 29.8, 29.7, 29.7, 29.6, 29.5, 29.4, 29.4, 29.3, 27.3, 27.2, 26.1, 26.1, 22.7, 14.1; ^{31}P NMR (162 MHz, $CDCl_3$) δ −0.48; HRMS (ESI-TOF) *m*/*z* $[M]^-$ calcd for $C_{42}H_{82}O_8P$ 745.5753, found 745.5754.

Data availability

All of the data are contained within the article.

Supporting information—This article contains supporting information.

Author contributions—S. D., V. Z. P., B. L. A., S. M. C., and J. S. writing–review and editing; S. D., T.-A. L., B. L. A., and J. S. writing–original draft; S. D., T.-A. L., O. I., V. Z. P., K. C. P., and K. C. visualization; S. D., T.-A. L., O. I., V. Z. P., K. C. P., and K. C. validation; S. D., T.-A. L., O. I., T. A., A. F., N. L., V. Z. P., K. C. P., K. C., B. L. A., S. M. C., and J. S. investigation; S. D., T.-A. L., V. Z. P., K. C. P., and K. C. formal analysis; S. D., T.-A. L., O. I., T. A., V. Z. P., K. C. P., K. C., B. L. A., S. M. C., and J. S. data curation; O. L., B. L. A., S. M. C., and J. S. supervision; O. I., B. L. A., and J. S. methodology; O. L., B. S. J. B., B. L. A., S. M. C., and J. S. funding acquisition; B. L. A., S, M. C., and J. S. resources; O. I., B. L. A., and J. S. conceptualization; J. S. project administration.

Funding and additional information—This work was supported by funds from the Ara Parseghian Medical Research Foundation (J. S., O. I., B. L. A., and S. M. C), the American Heart Association (J. S. and O. I.), and the U.S. National Institutes of Health R01 GM1125866 (J. S.) and NS114413 (S. M. C.). The content is solely the responsibility of the authors and does not necessarily represent the official views of the National Institutes of Health.

Conflict of interest—The authors declare that they have no conflicts of interest with the contents of this article.

Abbreviations—The abbreviations used are: BMP, bis-mono-acylglycerol phosphate; CH2Cl2, dichloromethane; LBPA,

lysobisphosphatidic acid; LE/LY, late endosome/late lysosome; LPG, lysophosphatidylglycerol; NPC, Niemann-Pick type C; PC, phosphatidylcholine; PG, phosphatidylglycerol; PLA2, phospholipase A2; THF, tetrahydrofuran.

References

1. Carstea, E. D., Morris, J. A., Coleman, K. G., Loftus, S. K., Zhang, D., Cummings, C., *et al.* (1997) Niemann-Pick C1 disease gene: homology to mediators of cholesterol homeostasis. *Science* **277**, 228–231
2. Naureckiene, S., Sleat, D. E., Lackland, H., Fensom, A., Vanier, M. T., Wattiaux, R., *et al.* (2000) Identification of HE1 as the second gene of niemann-pick C disease. *Science* **290**, 2298–2301
3. Chang, T.-Y., Reid, P. C., Sugii, S., Ohgami, N., Cruz, J. C., and Chang, C. C. Y. (2005) Niemann-Pick type C disease and intracellular cholesterol trafficking. *J. Biol. Chem.* **280**, 20917–20920
4. Kobayashi, T., Startchev, K., Whitney, A. J., and Gruenberg, J. (2001) Localization of lysobisphosphatidic acid-rich membrane domains in late endosomes. *Biol. Chem.* **382**, 483–485
5. Kobayashi, T., Beuchat, M.-H., Chevallier, J., Makino, A., Mayran, N., Escola, J.-M., *et al.* (2002) Separation and characterization of late endosomal membrane domains. *J. Biol. Chem.* **277**, 32157–32164
6. Kobayashi, T., Stang, E., Fang, K. S., de Moerloose, P., Parton, R. G., and Gruenberg, J. (1998) A lipid associated with the antiphospholipid syndrome regulates endosome structure and function. *Nature* **392**, 193–197
7. Kobayashi, T., Beuchat, M.-H., Lindsay, M., Frias, S., Palmiter, R. D., Sakuraba, H., *et al.* (1999) Late endosomal membranes rich in lysobisphosphatidic acid regulate cholesterol transport. *Nat. Cell Biol.* **1**, 113–118
8. Chevallier, J., Chamoun, Z., Jiang, G., Prestwich, G., Sakai, N., Matile, S., *et al.* (2008) Lysobisphosphatidic acid controls endosomal cholesterol levels. *J. Biol. Chem.* **283**, 27871–27880
9. McCauliff, L. A., Langan, A., Li, R., Ilnytska, O., Bose, D., Waghalter, M., *et al.* (2019) Intracellular cholesterol trafficking is dependent upon NPC2 interaction with lysobisphosphatidic acid. *eLife* **8**, e50832
10. Body, D. R., and Gray, G. M. (1967) The isolation and characterisation of phosphatidylglycerol and a structural isomer from pig lung. *Chem. Phys. Lipids* **1**, 254–263
11. Amidon, B., Brown, A., and Waite, M. (1996) Transacylase and phospholipases in the synthesis of bis(monoacylglycero)phosphate. *Biochemistry* **35**, 13995–14002
12. Medoh, U. N., Hims, A., Chen, J. Y., Ghoochani, A., Nyame, K., Dong, W., *et al.* (2023) The batten disease gene product CLN5 is the lysosomal bis(monoacylglycero)phosphate synthase. *Science* **381**, 1182–1189
13. Ito, M., Tchoua, U., Okamoto, M., and Tojo, H. (2002) Purification and properties of a phospholipase A2/lipase preferring phosphatidic acid, bis(monoacylglycerol) phosphate, and monoacylglycerol from rat testis. *J. Biol. Chem.* **277**, 43674–43681
14. Abe, A., Hinkovska-Galcheva, V., Bouchev, P., Bouley, R., and Shayman, J. A. (2024) The role of lysosomal phospholipase A2 in the catabolism of bis(monoacylglycerol)phosphate and association with phospholipidosis. *J. Lipid Res.* **65**, 100574
15. Cheruku, S. R., Xu, Z., Dutia, R., Lobel, P., and Storch, J. (2006) Mechanism of cholesterol transfer from the Niemann-pick type C2 protein to model membranes supports a role in lysosomal cholesterol transport. *J. Biol. Chem.* **281**, 31594–31604
16. Xu, Z., Farver, W., Kodukula, S., and Storch, J. (2008) Regulation of sterol transport between membranes and NPC2. *Biochemistry* **47**, 11134–11143
17. McCauliff, L. A., Xu, Z., Li, R., Kodukula, S., Ko, D. C., Scott, M. P., *et al.* (2015) Multiple surface regions on the Niemann-Pick C2 protein facilitate intracellular cholesterol transport. *J. Biol. Chem.* **290**, 27321–27331
18. Ilnytska, O., Lai, K., Gorshkov, K., Schultz, M. L., Tran, B. N., Jeziorek, M., *et al.* (2021) Enrichment of NPC1-deficient cells with the lipid LBPA stimulates autophagy, improves lysosomal function, and reduces cholesterol storage. *J. Biol. Chem.* **297**, 100813
19. Ilnytska, O., Jeziorek, M., Lai, K., Altan-Bonnet, N., Dobrowolski, R., and Storch, J. (2021) Lysobisphosphatidic acid (LBPA) enrichment promotes cholesterol egress via exosomes in Niemann pick type C1 deficient cells. *Biochim. Biophys. Acta Mol. Cell Biol. Lipids* **1866**, 158916
20. Vanier, M. T., Duthel, S., Rodriguez-Lafrasse, C., Pentchev, P., and Carstea, E. D. (1996) Genetic heterogeneity in Niemann-Pick C disease: a study using somatic cell hybridization and linkage analysis. *Am. J. Hum. Genet.* **58**, 118–125
21. Vanier, M. T. (2010) Niemann-Pick disease type C. *Orphanet J. Rare Dis.* **5**, 16
22. Luquain, C., Dolmazon, R., Enderlin, J.-M., Laugier, C., Lagarde, M., and Pageaux, J.-F. (2000) Bis(monoacylglycerol) phosphate in rat uterine stromal cells: structural characterization and specific esterification of docosahexaenoic acid. *Biochem. J.* **351**, 795
23. Besson, N., Hullin-Matsuda, F., Makino, A., Murate, M., Lagarde, M., Pageaux, J., *et al.* (2006) Selective incorporation of docosahexaenoic acid into lysobisphosphatidic acid in cultured THP-1 macrophages. *Lipids* **41**, 189–196
24. Bouvier, J., Zemski Berry, K. A., Hullin-Matsuda, F., Makino, A., Michaud, S., Geloën, A., *et al.* (2009) Selective decrease of bis(monoacylglycero)phosphate content in macrophages by high supplementation with docosahexaenoic acid. *J. Lipid Res.* **50**, 243–255
25. Amidon, B., Schmitt, J. D., Thuren, T., King, L., and Waite, M. (1995) Biosynthetic conversion of phosphatidylglycerol to sn-1:SN-1' bis(monoacylglycerol) phosphate in a macrophage-like cell line. *Biochemistry* **34**, 5554–5560
26. Hayakawa, T., Hirano, Y., Makino, A., Michaud, S., Lagarde, M., Pageaux, J. F., *et al.* (2006) Differential membrane packing of stereoisomers of bis(monoacylglycero)phosphate. *Biochemistry* **45**, 9198–9209
27. Brotherus, J., Renkonen, O., Herrmann, J., and Fischer, W. (1974) Novel stereoconfiguration in lyso-bis-phosphatidic acid of cultured BHK-cells. *Chem. Phys. Lipids* **13**, 178–182
28. Chinthapally, K., Blagg, B. S., and Ashfeld, B. L. (2022) Syntheses of symmetrical and unsymmetrical lysobisphosphatidic acid derivatives. *J. Org. Chem.* **87**, 10523–10530
29. Thornburg, T., Miller, C., Thuren, T., King, L., and Waite, M. (1991) Glycerol reorientation during the conversion of phosphatidylglycerol to bis(monoacylglycerol)phosphate in macrophage-like raw 264.7 cells. *J. Biol. Chem.* **266**, 6834–6840
30. Poorthuis, B. J., and Hostetler, K. Y. (1978) Conversion of diphosphatidylglycerol to bis(monoacylglyceryl)phosphate by lysosomes. *J. Lipid Res.* **19**, 309–315
31. Scherer, M., and Schmitz, G. (2011) Metabolism, function and mass spectrometric analysis of bis(monoacylglycero)phosphate and Cardiolipin. *Chem. Phys. Lipids* **164**, 556–562
32. Chen, J., Cazenave-Gassiot, A., Xu, Y., Piroli, P., Hwang, R., DeFreitas, L., *et al.* (2023) Lysosomal phospholipase A2 contributes to the biosynthesis of the atypical late endosome lipid bis(monoacylglycero)phosphate. *Commun. Biol.* **6**, 210
33. Joutti, A. (1979) The stereoconfiguration of newly formed molecules of bis(monoacylglycero)phosphate in BHK Cells. *Biochim. Biophys. Acta* **575**, 10–15
34. Shayman, J. A., Kelly, R., Kollmeyer, J., He, Y., and Abe, A. (2011) Group XV phospholipase A2, a lysosomal phospholipase A2. *Prog. Lipid Res.* **50**, 1–13
35. Weglicki, W. B., Ruth, R. C., and Owens, K. (1973) Changes in lipid composition of tritosomes during lysis. *Biochem. Biophysical Res. Commun.* **51**, 1077–1082
36. [preprint] Singh, S., Dransfeld, U., Ambaw, Y., Lopez-Scarim, J., Farese, R. V., and Walther, T. C. (2024) PLD3 and PLD4 synthesize S,S -BMP, a key phospholipid enabling lipid degradation in lysosomes. *bioRxiv*. https://doi.org/10.1101/2024.03.21.586175
37. Matsuo, H., Chevallier, J., Mayran, N., Le Blanc, I., Ferguson, C., Fauré, J., *et al.* (2004) Role of LBPA and Alix in multivesicular liposome formation and endosome organization. *Science* **303**, 531–534
38. Gruenberg, J. (2019) Life in the lumen: the Multivesicular endosome. *Traffic* **21**, 76–93

39. Walkley, S. U., and Vanier, M. T. (2009) Secondary lipid accumulation in lysosomal disease. *Biochim Biophys Acta* **1793**, 726–736
40. Vanier, M. T. (2014) Complex lipid trafficking in niemann-pick disease type C. *J. Inherit. Metab. Dis.* **38**, 187–199
41. Lieberman, A. P., Puertollano, R., Raben, N., Slaugenhaupt, S., Walkley, S. U., and Ballabio, A. (2012) Autophagy in lysosomal storage disorders. *Autophagy* **8**, 719–730
42. Menzies, F. M., Fleming, A., Caricasole, A., Bento, C. F., Andrews, S. P., Ashkenazi, A., *et al.* (2017) Autophagy and neurodegeneration: Pathogenic mechanisms and therapeutic opportunities. *Neuron* **93**, 1015–1034
43. Lee, J.-H., Yu, W. H., Kumar, A., Lee, S., Mohan, P. S., Peterhoff, C. M., *et al.* (2010) Lysosomal proteolysis and autophagy require presenilin 1 and are disrupted by alzheimer-related PS1 mutations. *Cell* **141**, 1146–1158
44. Menzies, F. M., Fleming, A., and Rubinsztein, D. C. (2015) Compromised autophagy and neurodegenerative diseases. *Nat. Rev. Neurosci.* **16**, 345–357
45. Grayson, M. (2016) Lysosomal storage disorders. *Nature* **537**, S145
46. Nixon, R. A. (2013) The role of autophagy in Neurodegenerative Disease. *Nat. Med.* **19**, 983–997
47. Storch, J., and Kleinfeld, A. M. (1986) Transfer of long-chain fluorescent free fatty acids between unilamellar vesicles. *Biochemistry* **25**, 1717–1726
48. McCauliff, L. A., and Storch, J. (2017) Transport assays for sterol-binding proteins: stopped-flow fluorescence methods for investigating intracellular cholesterol transport mechanisms of NPC2 protein. *Methods Mol. Biol.* **1583**, 97–110
49. Pipalia, N. H., Saad, S. Z., Subramanian, K., Cross, A., al-Motawa, A., Garg, K., *et al.* (2021) Hsp90 inhibitors reduce cholesterol storage in Niemann-Pick Type C1 mutant fibroblasts. *J. Lipid Res.* **62**, 100114
50. Vacca, F., Vossio, S., Mercier, V., Moreau, D., Johnson, S., Scott, C. C., *et al.* (2019) Cyclodextrin triggers MCOLN1-dependent endo-lysosome secretion in Niemann-Pick Type C cells. *J. Lipid Res.* **60**, 832–843
51. Chen, H., Zhang, H., McCallum, C. M., Szoka, F. C., and Guo, X. (2007) Unsaturated cationic ortho esters for endosome permeation in gene delivery. *J. Med. Chem.* **50**, 4269–4278
52. Abe, M., Sawada, Y., Uno, S., Chigasaki, S., Oku, M., Sakai, Y., *et al.* (2017) Role of acyl chain composition of phosphatidylcholine in Tafazzin-mediated remodeling of cardiolipin in liposomes. *Biochemistry* **56**, 6268–6280
53. Sato, S., Kawamoto, J., Sato, S. B., Watanabe, B., Hiratake, J., Esaki, N., *et al.* (2012) Occurrence of a bacterial membrane Microdomain at the cell division site enriched in phospholipids with polyunsaturated hydrocarbon chains. *J. Biol. Chem.* **287**, 24113–24121
54. Rowland, M. M., and Best, M. D. (2009) Modular synthesis of bis(monoacylglycero)phosphate for convenient access to analogues bearing hydrocarbon and perdeuterated acyl chains of varying length. *Tetrahedron* **65**, 6844–6849